POLITECNICO
MILANO 1863

SCUOLA DI INGEGNERIA INDUSTRIALE
E DELL'INFORMAZIONE

EXECUTIVE SUMMARY OF THE THESIS

SIMULATION AND VALIDATION USING HIL TECHNIQUE OF THE CONTROL SYSTEM OF A LIGHT TRAIN POWERED BY HYDROGEN FUEL CELLS AND BATTERIES

TESI MAGISTRALE IN ELECTRICAL ENGINEERING – INGEGNERIA ELETTRICA

AUTHOR: Francesco MAGGIULLI

ADVISOR: Giovanni Maria FOGLIA

ACADEMIC YEAR: 2021-2022

1. Preface

The international goal of governments is to reduce the environmental impact of fossil fuels and prefer sustainable sources. One of the main problems in the railway world is the presence of trains that use a diesel engine to run on certain routes. These types of trains are used where there is still no electrified railway network. The main reason is the high infrastructure costs. In this thesis, a non-electrified route, the St Ives Bay Line Railway, South West of the UK, will be taken as a sample. The diesel train which still runs on it will be taken as a model, and it will be investigated how to replace it by using a power supply consisting of Hydrogen Fuel Cells (FCs) and Li-ion batteries. The choice of these two lies in the amount of energy and power available. Fuel cells have a higher energy density than batteries, in opposition, batteries can release much more power than fuel cells. Since the fuel cells are the main power supply and batteries are sized as an auxiliary, we need two complementary sources to run in every conditions. The setup used even today for fuel cells is bulky and heavy [4]. A new layout had to be designed to make the train suitable and useful for our aims.

What differentiates this thesis is the use of the Hardware-in-the-loop simulation technique, with "Typhoon HIL" simulator, which differs from a normal simulation because some components are not virtual but real. The real component that we used is the microcontroller, which is the brain of the project. The components that remain simulated are the motor, the inverters, and the sources. Basically, we developed the algorithm which the microcontroller has to execute. Through a physical connection to the simulator, it was possible to control the inverters [3] and consequently decide how much power send to the motor.

2. Setup

The heart of the project lies in the type of motor used, which is a double three-phase permanent

magnet motor (DTPMSM). It can be powered from two separate sources via the two different windings. We can therefore change the normal setup by removing components that are no longer used (DC link between different sources[4]). The setup (Figure 1) was studied by my colleague Nursaid Polater on a commission from Dr Pietro Tricoli [1]. It is composed by the two sources, the two inverters and the motor.

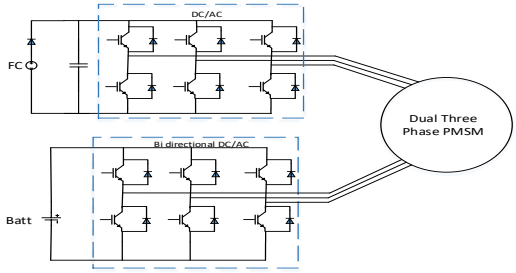

Figure 1 : New Setup Studied [1]

The advantages to use this configuration are several and they are summarized in Table 1[1].

Parameters	Standard Setup	Proposed Setup
Volume$[dm^3]$	**1.15e3**	**321**
Weight$[kg]$	**96.23**	**1.05**
Energy$[J]$	**16.09**	**3.83**
Power$[kVA]$	**1042.8**	**786.4**
Cost [£]	**6369.59**	**853.97**

Table 1 : Comparison between the Standard and the Proposed Configurations.

3. Motor and its Equations

The motor is the heart of the design, thanks to which two sources can be used separately, whereas the two windings are treated as electrically separate. In reality, the two windings suffer from a mutual contribution between one and the other. Let us therefore schematize the motor and write down its main equations. Figure 2 show that the permanent magnets are positioned on the rotor. The stator, on the other hand, has the two windings displaced by 30° from each other. The choice of this type of motor is also due to the fact that the phase shift of 30° can reduce oscillations in torque. Using the Clark transform, we can model the motor through the use of reference axes. By choosing axes that are fixed with the rotor, the motor schematic becomes as in Figure 3.

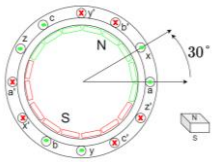

Figure 2 : Motor Diagram

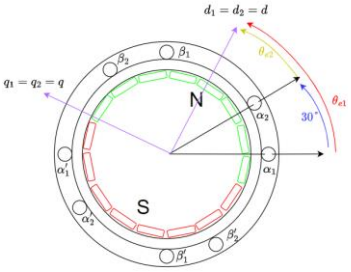

Figure 3 : $d-q$ Axis Reference Frame

The stator and mechanical equations that we can perform by the study of this motor scheme are (p indicated the time derivative) [1]:

$$v_{d1} = R_s i_{d1} + L_d p i_{d1} + M_d p i_{d2} - \Omega_m L_q i_{q1} - \Omega_m M_q i_{q2}$$
$$v_{d2} = R_s i_{d2} + L_d p i_{d2} + M_d p i_{d1} - \Omega_m L_q i_{q2} - \Omega_m M_q i_{q1}$$
$$v_{q1} = R_s i_{q1} + L_q p i_{q1} + M_q p i_{q2} + \Omega_m L_d i_{d1} + \Omega_m M_d i_{d2} + \Omega_m \psi_{pm}$$
$$v_{q2} = R_s i_{q2} + L_q p i_{q2} + M_q p i_{q1} + \Omega_m L_d i_{d2} + \Omega_m M_d i_{d1} + \Omega_m \psi_{pm}$$
$$T_e = \frac{3}{2} n_p \psi_{pm} (i_{q1} + i_{q2})$$
$$T_e - T_r = J_{eq} * \frac{d}{dt}\Omega_m + \beta \Omega_m$$

(Eq. 1)

The mass of the train is $m_t = 150[tons]$, the train has four carriage and two motors for each which means that each motor should be sized for a mass $m_m = 18.75[tons]$. The train incurs in resistance due to the friction with the air or by the wheels and the rail. To calculate this resistance force, we used the Davis equation, an empirical formula which takes care about all the resistive contributions.

$$R[N] = A + B * v + C * v^2 + m_m * g * grad$$

(Eq. 2)

Where A, B, C are the Davis Coefficients, $v\left[\frac{m}{s}\right]$ is the speed, $g\left[\frac{m}{s^2}\right]$ is the gravity acceleration and $grad[‰]$ is the gradient of the terrain. Since R is a force, we need to convert it to a torque.

$$T[Nm] = R[N] * \frac{d_w/2}{g_r}$$

(Eq. 3)

Where $d_w[m] = 1[m]$ is the wheel diameter and $g_r = 6$ is the gear ratio.

The FCs are sized to perform the nominal resistant torque at the nominal speed. Since the nominal speed is 157 $\left[\frac{rad}{s}\right]$, the nominal resistant toque from the Davis equation is about $188[Nm]$. We consider

$T_{rn} = 200[Nm]$. The inertia of the train translated to one motor is $J_{eq} = 147.135[kgm^2]$. The motor chosen has a nominal toque of $T_n = 750[Nm]$ and maximum of $T_{max} = 850[Nm]$. Under these conditions we can say that the acceleration is about

$$a = \frac{850[Nm] - 200[Nm]}{147.135[kgm^2]} \approx 4.4\left[\frac{rad}{s^2}\right]$$

(Eq. 4)

The power performed by the motor is $P_t = 120[kW]$. Its parameters are reported in Table 2.

The power of the Fuel Cell is:

$$P_{FC} = T_{rn} * \Omega_n = 31.4[kW]$$

(Eq. 5)

As consequence, the batteries power is:

$$P_{batt} = P_t - P_{FC} = 88.6[kW]$$

(Eq. 6)

Data	Value
n_p	2
$T_n - T_{max}$	$750[Nm] - 850[Nm]$
Ω_n	$157[rad/s]$
P_n	$120[kW]$
V_n	$359[V]$
η	96.4%
$cos\varphi$	0.96
I_{pRMS}	$201[A]$
R_s	$0.0088[\Omega]$
$L_a = L_b$	$0.897[mH]$
L_{ls}	$0.207[mH]$
J_M	$1.065[kgm^2]$
J_{eq}	$147.135[kgm^2]$
β	$0.094\left[\frac{kgm^2}{s}\right]$
ψ_{pm}	$0.97[Wb]$

Table 2 : Motor Parameters [1]

4. FOC Scheme and Logical Diagram

By studying the motor equations, we can deduce how the motor can be controlled in the best possible way. First of all, the electromagnetic torque, which is what the motor can produce, depends linearly on the sum of the quadrature currents(Eq. 1). Consequently, the currents on the direct axis, since they don't have a useful contribution, will be set to zero to allow use of the maximum quadrature current in the torque. Therefore, a scheme to control the motor called Field-Oriented-Control (FOC) was created. It has as input the desired speed, through a process, by using the motor equations and PI controllers, transforms this setpoint into stator currents and voltages to push a desired torque and accelerate the motor. The scheme is reported in Figure 4.

It is possible to distinguish two loops, an internal one which controls the currents and an external which controls the speed.
In the FOC scheme there is a Power Sharing block after the speed controller. It is crucial for the running of the train since the two windings are supplied by two different sources. In fact, the batteries help the fuel cell mainly during the acceleration phases and recover energy when the braking is needed. Moreover, it limits the state of charge (SOC) of the batteries between 20% and 80%. The logical diagram which is integrated in the power sharing block is reported in Figure 5.

5. Experimental Data

We performed a simulation by running the train between five stations on the St. Ives Bay Line, starting from St. Erth, until St. Ives and come back to the initial one. The five stations are placed at different distance between them (Table 3, total track is $13.4[km]$) and moreover they have different limit speed and gradient of the terrain.

Station	Distance from begin [m]
St. Erth	0
Lelant Salting	1020
Lelant	1731
Carbis Bay	4820
St. Ives	6700

Table 3 : Stations Position for the St Ives Bay Line

We need to tune the PI parameters. We have five PI controllers. One follows the mechanical speed equation, the other four follow the dynamics of the direct and quadrature axis currents. Since we are using an isotropic motor, the dynamics of the currents are the same, we only need to study the parameters once for all four controllers. They must also be calibrated by taking into account the slope of the terrain, which adds a gradient resistant torque to the Davis equation. The slope of the terrain is shown in Figure 6. It is subject to rapid changes, which implies a higher condition for parameter adjustment, as a control is required that is able to execute the fixed speed without losing control.

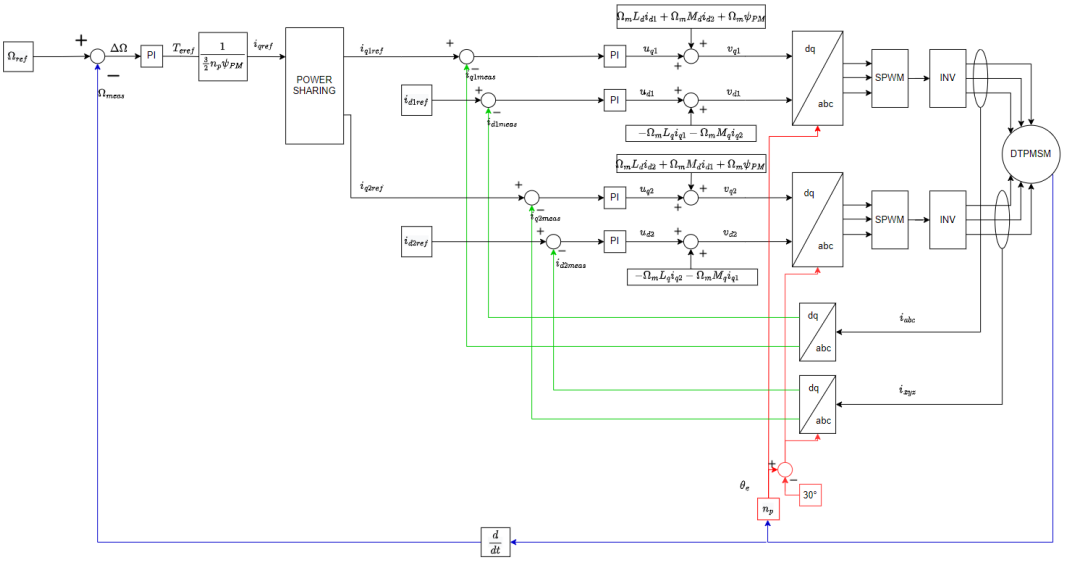

Figure 4 : FOC Scheme

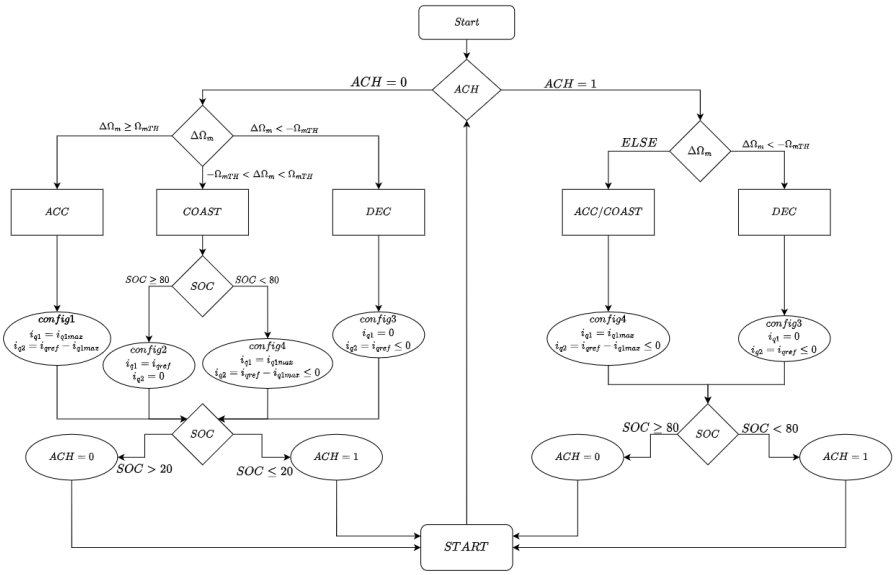

Figure 5 : Logic Scheme of the Power Sharing Block

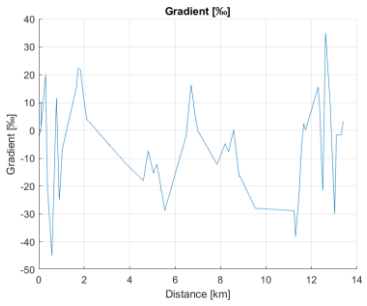

Figure 6 : Gradient of the Track

In addition, the logic scheme must also be monitored, as rapid switching between configurations occurs due to the high slope, resulting in current steps and thus electromagnetic torque steps. This condition can be mitigated by a retarding hysteresis function, which allows the system dynamics to be slowed down and the microcontroller to decide the right current under more stable system conditions.

The gain parameters of the PIs controller are calculated based on the transfer function of the stator equations. In particular the mechanical and current transfer functions in the Laplace domain are:

$$G_m(s) = \frac{1}{J_{eq}s + \beta}$$

$$G_i(s) = \frac{1}{L_s s + R_s}$$

(Eq. 7)

By setting the mechanical time constant $\tau_m = 0.5[s]$ and the electrical one, 100 times faster $\tau_e = 5[ms]$, we obtain the gain parameters [2]:

$$Speed\ Regulator \begin{cases} k_p = 362.488 \\ k_i = 18.2278 \end{cases}$$

$$Current\ \ Regulators \begin{cases} k_p = 1.2833 \\ k_i = 6.4524 \end{cases}$$

(Eq. 8)

With these parameter values, the step responses of both the mechanical and the electrical transfer functions are good: they do not have overshoot and reach the steady state in the expected time.

We will illustrate the results obtained from the simulation performed on the entire track. The journey last about 25 minutes. The parameters we are mostly interested in is the speed profile. It is shown in Figure 7. We can observe that during the acceleration and deceleration phases, the reference is followed with a good approximation. But after Lelant and St. Ives, there is a displacement. This phenomenon is due to the slope of the terrain. We size the motor with a maximum torque $T_{max} = 850[Nm]$to accelerate at more than 4.4 $\left[\frac{rad}{s^2}\right]$. In these cases, instead, the resistant torque is more than the nominal one. For this reason, the acceleration achieved is about 60% of the nominal. To better understand this concept

Figure 8 shows the total resistance torque (top) evaluated by the Davis Equation, and its two contributions, that is the resistance due to the air and wheel drag (middle) and to the slope (bottom).

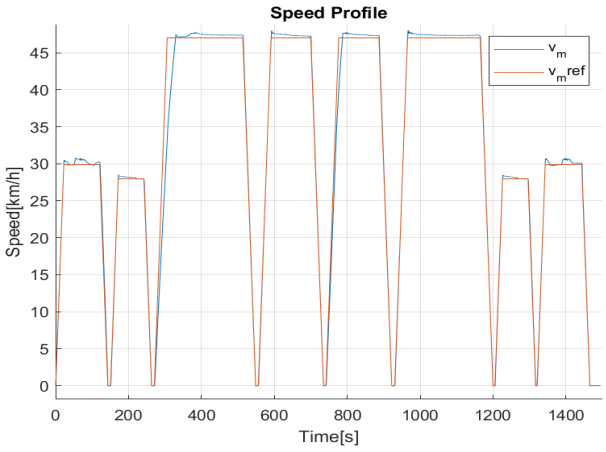

Figure 7 : Speed Profile

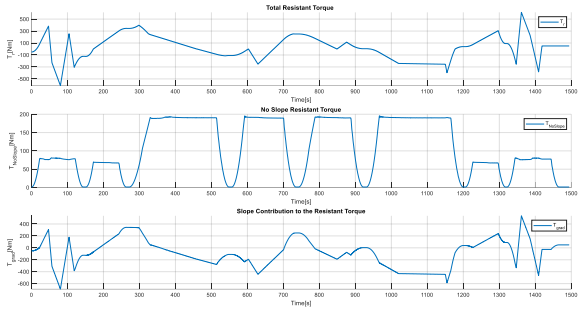

Figure 8 : Contributions of the Resistant Torque

Figure 11 shows the torque profile, in particular the electromagnetic torque T_e and the resistant one T_r. The time intervals when the electromagnetic torque is higher or lower than the resistant, define the acceleration or deceleration whereas when $T_e = T_r$ identifies the coasting phases. The maximum torque is not always reached since the resistant torque participates in both the acceleration (when is negative) and braking (positive) of the train and the acceleration is limited. Furthermore, in the coasting phases, the resistant torque is followed by the electromagnetic torque with a good approximation.

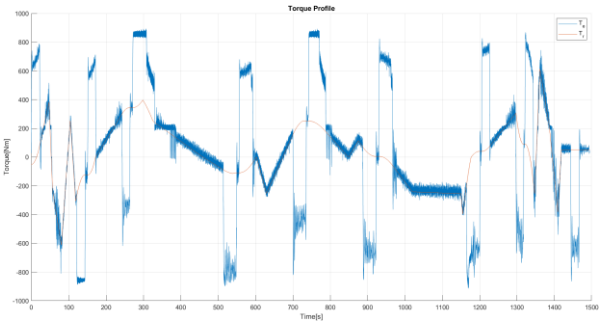

Figure 9 : Torque Profile

The Figure 10 and Figure 11 show the behavior of the direct and quadrature currents of the first and second windings respectively. We are interested in the quadrature currents. The value in the first winding is mostly 70[A] with some minor intervals where it becomes zero (mainly during deceleration). On the second, however, the behavior changes a lot because the batteries have a complementary role respect to the FCs. In fact, the function of the batteries is to help when the FCs are unable to power the motor as required due to the gradient.

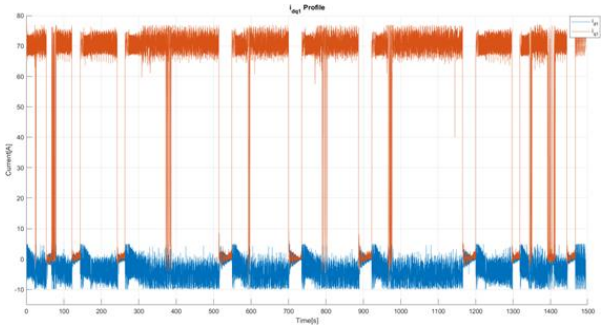

Figure 10 : First Winding Currents

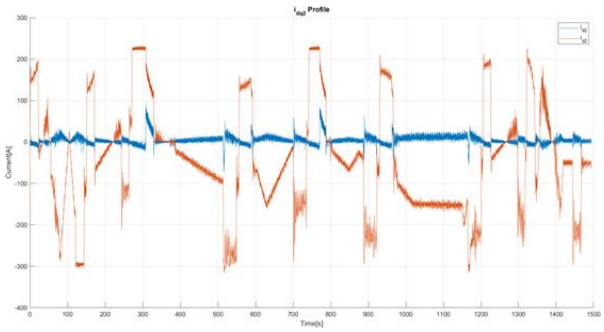

Figure 11 : Second Winding Currents

Another interesting parameter concerns the state of battery charge (SOC) in Figure 12. In the nominal condition it starts at 50% and reaches about 67% at the end of the trip. If we look at the current in the second winding, it remains negative for most of the journey because it is recharged by the fuel cell and the gradient is predominantly negative. These conditions allow a huge amount of energy to be recovered during an entire journey.

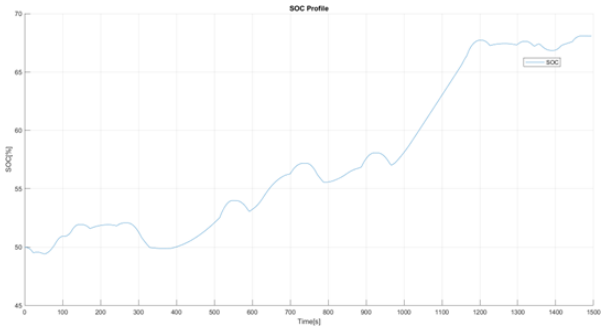

Figure 12 : SOC Profile

At the end of the study, we checked the power performed by the two winding in Figure 13. In the first one it reaches 31.4$[kW]$. Instead, the second one has peak of 75$[kW]$ in acceleration and about 120$[kW]$ in breaking conditions. This confirms that the moto size is 120$[kW]$.

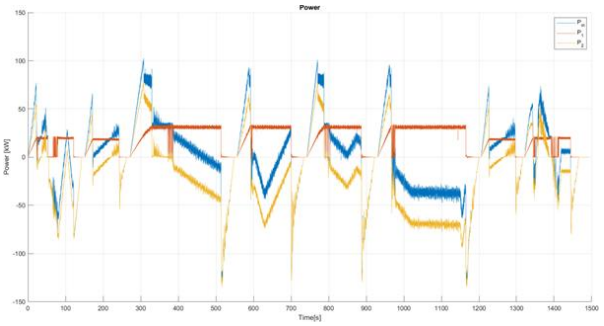

Figure 13 : Power Profile

6. Conclusion

The objective of this thesis was to simulate a new light train setup suitable to replace soon the diesel-powered ones that are still present on some non-electrified routes. Furthermore, through the hardware-in-the-loop technique, we were able to validate the results by confirming the feasibility of this configuration. Very promising results were obtained. We verified that the choice of hydrogen fuel cells and li-ion batteries, being complementary in energy and power, can be used in multiple scenarios by adapting their function to the context and operating conditions. The results obtained were made possible using a three-phase dual motor with permanent magnets. In this work, we assumed that the rotor angle is given directly by the simulator; future developments include the study of a sensor less control. Another aspect concerns the logic scheme. As we have seen, the SOC of the batteries grows and increases during the journey. It will therefore be possible to modify the logic scheme to utilize the batteries much more than we scheduled. A final point must be made about the unbalanced degradation of the two windings. This is due to the fact that the powers delivered by the sources are different, leading to greater degradation in the second than in the first. To remedy this, a exchange between the two windings may be necessary, which will be repeated cyclically. The exchange period can be calculated through the energies or current RMS value of the two windings. In conclusion, we were able to obtain an interesting result regarding the railway development of new systems. We are confident that this study can bring benefits in terms of the environment and the advancement of technology in the railway industry.

7. References

[1] Nursaid Polater, Pietro Tricoli, Stuart Hillmansen "Analysis, Development and Control of Fuel Cell Propulsion System for Light Railways"

[2] Francesco Castelli Dezza, Calzoni Pietro, “Modellistica e progetto di regolatori pi e pid orientati allo sviluppo su microcontrollore”

[3] Giovanni Maria Foglia, “Power Electronic”, his notes from the course 2020-2021

[4] Morris Brenna, Federica Foiadelli, Dario Zaninelli, Electrical Railway Transportation Systems, New Jersey: IEEE Press Wiley, 2018.

8. Acknowledgements

Vorrei ringraziare innanzitutto il relatore di questa tesi, il prof. Foglia, per la sua organizzazione, la sua professionalità e la sua pazienza.
Ringrazio il Dr. Tricoli per avermi permesso di sviluppare un suo progetto e con esso anche le persone che a Birmingham mi sono state vicine, Nursaid, Tabish e Jovan.
Vorrei ringraziare i miei compagni di studi e del gruppo “Delta di Dirac”, avete reso gli anni di politecnico un po’ meno difficili. Con essi anche i miei amici più cari di Longuelo che mi hanno incitato nel mio percorso.
Un sentito ringraziamento alla mia famiglia, ai miei genitori, le mie sorelle, mio nonno, mia zia, Luchino e Gaia per esserci sempre stati, aver supportato tutte le mie stranezze, e reso la persona che sono.